Prediction of Colorectal Cancer Liver Metastasis through an MRI Radiomic Model

Yaokun Wu , Ning Liu , Yunyun Tao , Jing Zheng , Xiaohua Huang , Lin Yang * , Xiaoming Zhang

Posted Date: 29 December 2023

doi: 10.20944/preprints202312.2320.v1

Keywords: Radiomics; MRI; Colorectal cancer; Liver Metastasis

Article

Prediction of Colorectal Cancer Liver Metastasis through an MRI Radiomic Model

Yao-Kun Wu [1,2], Ning Liu [1,3], Yun-Yun Tao [1], Jing Zheng [1], Xiao-Hua Huang [1], Lin Yang [1,*] and Xiao-Ming Zhang [1]

[1] Medical Imaging Key Laboratory of Sichuan Province; Interventional Medicine Center, Department of Radiology, Medical Research Center, Affiliated Hospital of North Sichuan Medical College, Nanchong, Sichuan 637000, P. R. China
[2] Department of Radiology, the Third Hospital of Mianyang.Sichuan Mental Health Center, Mianyang, Sichuan 621000, P. R. China
[3] Hospital of Chengdu Office of People's Government of Tibetan Autonomous Region (Hospital. C.T.), Chengdu 610041, P. R. China
* Correspondence: linyangmd@163.com

Abstract: Objective: To investigate the efficacy of a magnetic resonance imaging (MRI) radiomics model in predicting colorectal cancer liver metastasis (CRLM). **Methods:** A total of 120 patients who underwent baseline MRI examination at the Affiliated Hospital of North Sichuan Medical College from June 2016 to August 2022 and were pathologically confirmed to have colorectal cancer (CRC) were randomly divided into a training group and a validation group. The clinical risk factors and MRI data of all patients were collected. Univariate and multivariate analysis were used to screen the clinically independent risk factors for CRLM. The radiomic features of each sequence were extracted from oblique axial or axial fat-free T_2-weighted imaging (T_2WI) and diffusion-weighted imaging (DWI) sequences. Least absolute shrinkage and selection operator (LASSO) regression was used to screen the optimal radiomic features of each sequence. Logistic regression was used to establish a prediction model of each sequence (T_2WI and DWI models), a combined radiomics model (M) integrating the features of T_2WI and DWI sequences, and a combined imaging-clinical model (U) combining the radiomic features of each sequence with clinically independent risk factors. The area under the receiver operating characteristic curve (AUC) was calculated to evaluate the predictive performance of each model. **Results:** Among the 120 CRC patients enrolled, 57 had liver metastasis, and 63 did not. The tumor markers carcinoembryonic antigen and carbohydrate antigen 19-9 were clinically independent risk factors for CRLM. Three optimal radiomic features were screened from T_2WI and DWI sequences through LASSO regression analysis, respectively. The AUC values of the T_2WI, DWI, M, and U models were 0.811, 0.803, 0.824, and 0.899 in the training group and 0.795, 0.798, 0.813, and 0.889 in the validation group, respectively. The predictive performance of the combined models was better than that of the single-sequence models. The U model performed best at predicting CRLM. **Conclusion:** An MRI radiomics model based on CRC primary lesions can predict CRLM well. Our combined model integrating the radiomic features of each sequence and clinically independent risk factors had the best predictive performance.

Keywords: radiomics; MRI; colorectal cancer; liver metastasis

1. Introduction

Colorectal cancer (CRC) is a common malignant tumor of the gastrointestinal tract [1]. Globally, CRC ranks third in incidence among malignant tumors [2–5] and is the third leading cause of cancer-related deaths [1,6]. There are more than 1,800,000 new cases of CRC each year [2] and approximately 900,000 deaths [2,7]. Even more worryingly, the incidence of CRC is increasing, especially in the young population [1]. Studies have shown that up to 20% of CRC patients have metastases when initially diagnosed [7], and approximately 50% of patients who receive radical surgical treatment will

 doi:10.20944/preprints202312.2320.v1

also develop metastasis within 5 years [8]. Because mesentery blood drains into the hepatic portal system, the liver is the most common organ involved in the hematogenous metastasis of CRC [3,4,9–11]. Liver metastasis (LM) is the leading cause of death in CRC patients [4,9,10, and the median survival of untreated colorectal liver metastases (CRLM) patients is only 6.9 months [9,10]; furthermore, the 5-year survival rate is <5% [10]. However, for patients who undergo radical resection for LM or who achieve no evidence of disease (NED), the median survival time increases to 35 months, and the 5-year survival rate increases to 30-57%. [9,10 Therefore, early detection and active treatment of LM are highly important for improving the prognosis of CRC patients. Traditional imaging methods have been widely used in the preoperative clinical assessment of CRLM; however, their diagnostic accuracy is still unsatisfactory [12,13]. Although some clinicopathological features can be used to assess the potential risk of CRLM, these indicators can be obtained only after radical resection [14–16]. Therefore, there is an urgent clinical need for noninvasive and accurate preoperative prediction of CRLM.

The concept of radiomics was first proposed by Lambin et al. in 2012 [17], who mined and extracted a large amount of quantitative features from existing image data [18,19. Subsequently, analytical methods such as machine learning were used with radiomics to achieve disease classification and prognosis prediction [20–25]. Currently, magnetic resonance imaging (MRI) is the preferred method for the clinical assessment of CRLM; among the various MRI modalities, T2-weighted imaging (T2WI) and diffusion-weighted imaging (DWI) sequences obtained via axial MRI are key for finely annotating CRC. However, to date, very few studies have investigated the ability of MR T2WI and DWI-based radiomic models to predict CRLM. This study investigated the performance in predicting LM by a radiomic model based on baseline MR T2W1 and DWI sequences of CRC primary lesions.

2. Results

2.1. Patient Characteristics

A total of 120 patients were enrolled in the study, including 85 males and 35 females; the age of the patients ranged from 25 to 88 years, and the mean age was 61.06±12.83 years. There were 93 patients with rectal cancer (RC) and 27 patients with colon cancer (CC). Among all the patients, 57 developed LM by the follow-up date, while 63 did not develop. The patients were randomly divided into a training group (83 patients) and a validation group (37 patients) at a ratio of 7:3. The results of univariate and multivariate analyses of the clinical characteristics revealed significant differences in carcinoembryonic antigen (CEA) and carbohydrate antigen 19-9 (CA19-9) levels between the LM group and the non-LM group (P <0.05) (Table 2).

Table 2. Clinical features of patients with CRLM(+) and CRLM(-) in the training and validation cohorts.

	Training			Validation		
	CRLM(+) (n =39)	CRLM(-) (n =44)	P value	CRLM(+) (n =18)	CRLM(-) (n =19)	P value
Age/yr (Mean±SD)	64.97±11.76	59.50±12.89	0.052	60.06±13.95	57.58±12.73	0.565
Sex (%)			0.228			0.419
Male	28(71.8)	26(59.1)		16(88.9)	15(78.9)	
Female	11(28.2)	18(40.9)		2(11.1)	4(21.1)	
MRT stage (%)			0.988			0.810
T1	0(0)	1(2.3)		0(0)	0(0)	
T2	0(0)	9(20.5)		1(5.6)	2(10.5)	

 doi:10.20944/preprints202312.2320.v1

T3	26(66.7)	24(54.5)		11(61.1)	10(52.6)	
T4	13(33.3)	10(22.7)		6(33.3)	7(36.8)	
MRN stage (%)			0.887			0.890
N0	8(20.5)	11(25.0)		5(27.8)	6(31.6)	
N1	11(28.2)	12(27.3)		5(27.8)	4(21.0)	
N2	20(51.3)	21(47.7)		8(44.4)	9(47.4)	
CEA level (%)			<0.001			0.001
Normal	7(17.9)	31(70.5)		2(11.1)	14(73.7)	
Elevated	32(82.1)	13(29.5)		16(88.9)	5(26.3)	
CA19-9 level (%)			<0.001			0.999
Normal	19(48.7)	42(95.5)		9(50.0)	19(100)	
Elevated	20(51.3)	2(4.5)		9(50.0)	0(0)	

Notes: CRLM, colorectal cancer liver metastasis; CEA, carcinoembryonic antigen; CA19-9, carbohydrate antigen 19-9.

2.2. Feature Extraction and Selection

A total of 352 features were extracted from the T2W and DW datasets, and features with an ICC<0.75 were excluded. Based on these findings, 38 features were excluded in the T2WI dataset (8 features were excluded by the intragroup consistency test, 36 features were excluded by the intergroup consistency test, and 6 features were duplicated within and between groups), while a total of 19 features were excluded from the DWI dataset (5 features were excluded by the intragroup consistency test, 19 features were excluded by the intergroup consistency test, and 5 features were duplicated within and between groups). For the radiomic features screened by the intragroup and intergroup consistency tests, the independent sample *t* test or *Mann–Whitney U* test was used to further exclude 20 and 64 features from the T2WI and DWI datasets, respectively, leaving 294 and 269 features that were statistically significant (P <0.05). Finally, LASSO regression analysis yielded 3 and 3 optimal features, respectively, from the statistically significant omics features (Table 3) (Figures 3–5).

Table 3. Selected features predictive of CRLM.

Prediction model	Feature category		CRLM (+) vs. CRLM (-)
T_2WI model	Texture features	GLCM	X0.4 Inverse Variance
	Shape features	Shape	Compactness 1
			Max3D Diameter
DWI model	Texture features	GLCM	X45.7 Information MeasureCorr1
			X135.7 Information MeasureCorr1
	Shape features	Shape	Max3D Diameter

Notes: CRLM, colorectal cancer liver metastasis; GLCM, gray-level co-occurrence matrix; GLCM features were constructed in four directions (θ = 0°, 45°, 90°, and 135°) and three offsets (d = 1, 4, 7).

 doi:10.20944/preprints202312.2320.v1

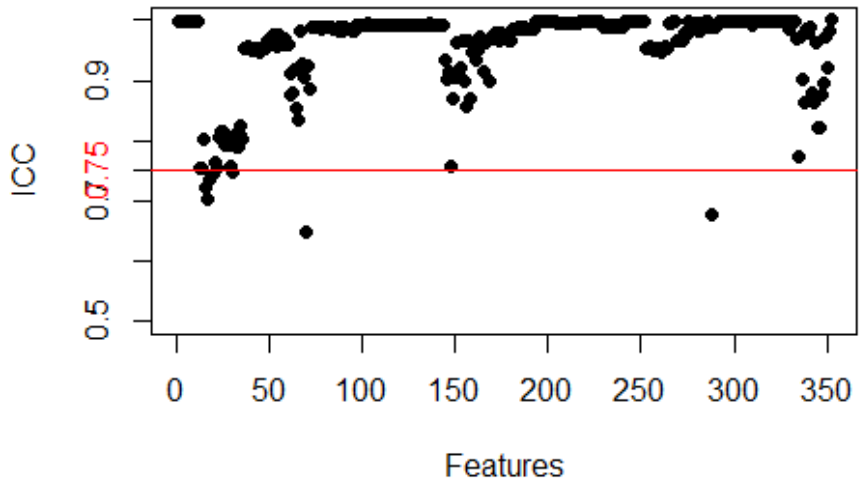

A

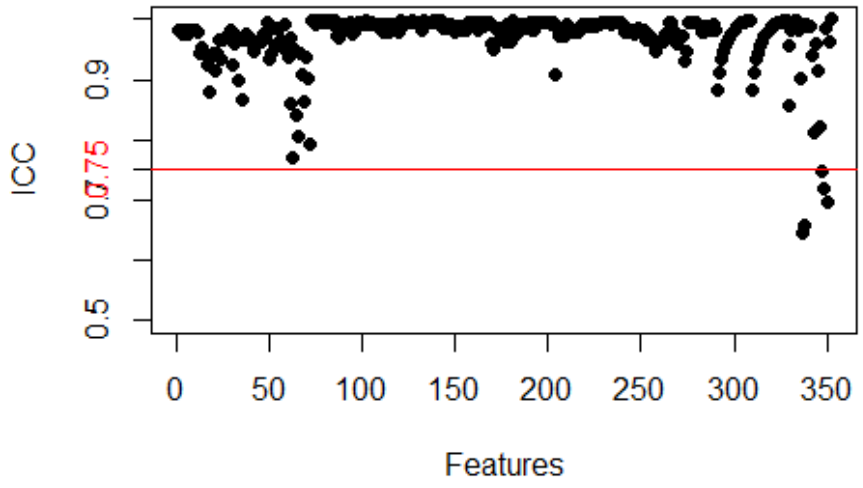

B

Figure 3. Intragroup consistency test: evaluation of the repeatability of MRI radiomic feature extraction by the intraclass correlation coefficient (ICC). (A) T_2-weighted imaging features; (B) Diffusion-weighted imaging features.

 doi:10.20944/preprints202312.2320.v1

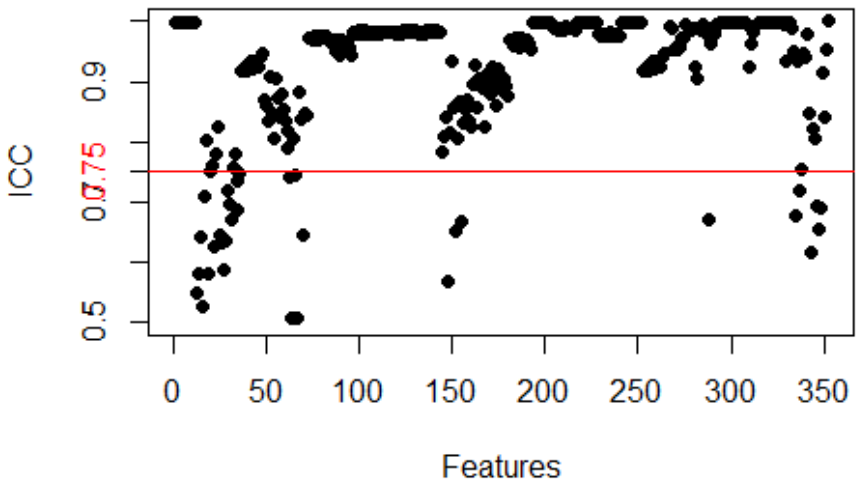

A

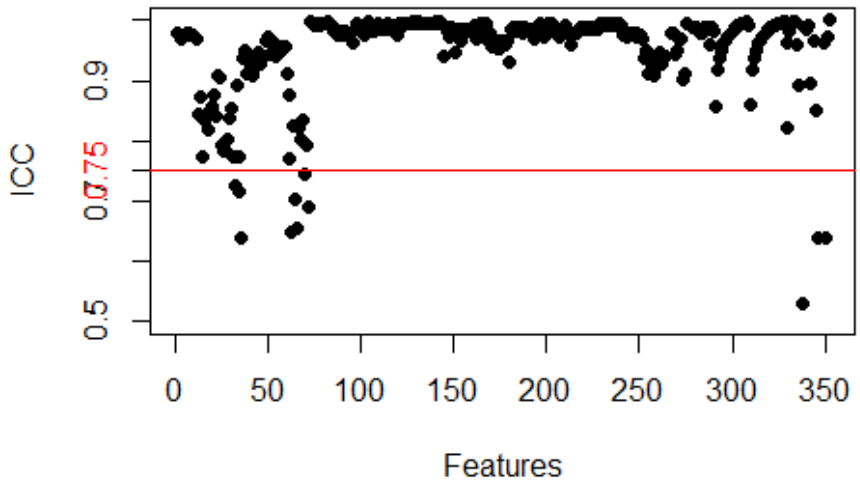

B

Figure 4. Intergroup consistency test: evaluation of the repeatability of MRI radiomic feature extraction by the intraclass correlation coefficient (ICC). (A) T_2-weighted imaging; (B) Diffusion-weighted imaging.

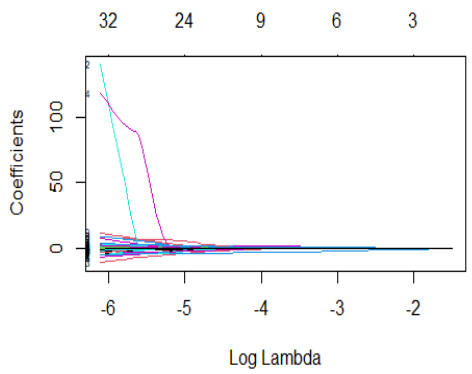

A1

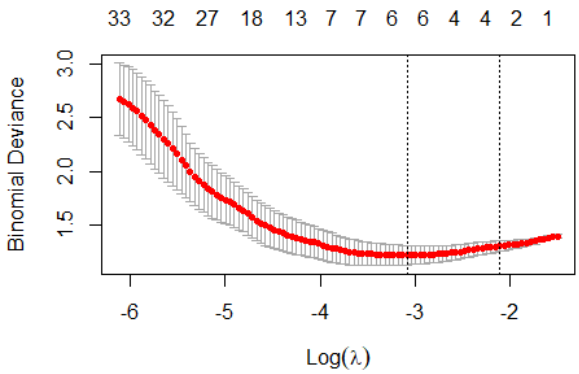

A2

 doi:10.20944/preprints202312.2320.v1

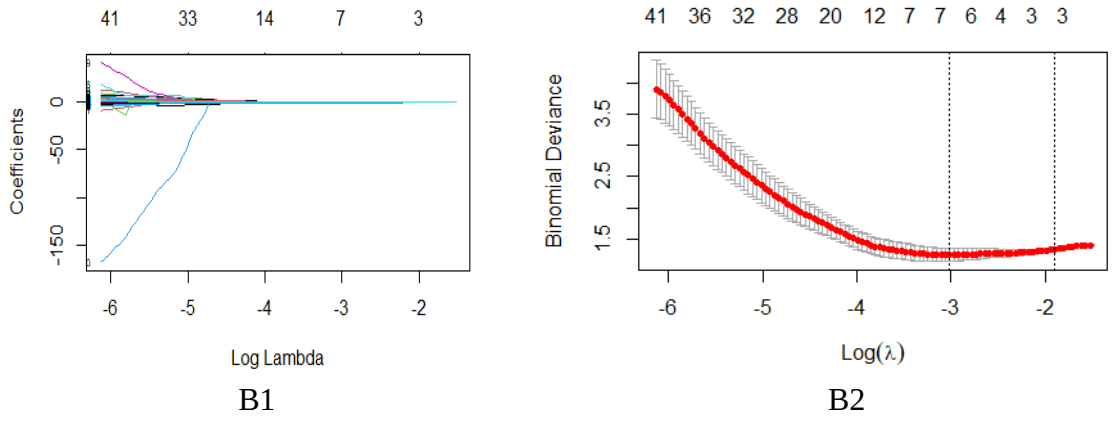

B1 B2

Figure 5. Feature selection using least absolute shrinkage and selection operator (LASSO) regression to predict CRLM. (A1-A2) T_2-weighted imaging. (B1-B2) Diffusion-weighted imaging.

2.3. Model evaluation

The area under the curve (AUC) values of the T2WI, DWI, M, and U models were 0.811, 0.803, 0.824, and 0.899, respectively, in the training cohort and 0.795, 0.798, 0.813, and 0.889, respectively, in the validation cohort. Among them, the combined clinical-radiomics model (the U model) performed the best in predicting CRLM (Table 4, Figure 6).

Table 4. Performance of the constructed models in predicting CRLM.

Cohort	Prediction model	AUC	Sen	Spe	PPV	NPV	ACC	F1-score
Training cohort								
	T_2WI model	0.811	0.795	0.718	0.761	0.757	0.759	0.778
	DWI model	0.803	0.750	0.769	0.786	0.732	0.759	0.767
	M model	0.824	0.773	0.769	0.791	0.750	0.771	0.782
	U model	0.899	0.795	0.744	0.778	0.763	0.772	0.787
Validation cohort								
	T_2WI model	0.795	0.842	0.778	0.800	0.824	0.811	0.821
	DWI model	0.798	0.737	0.778	0.778	0.737	0.757	0.757
	M model	0.813	0.789	0.778	0.789	0.778	0.784	0.789
	U model	0.889	0.895	0.833	0.850	0.882	0.865	0.872

Notes: CRLM, colorectal cancer liver metastasis; M model, multisequence radiomic model; U model, union of the multisequence radiomic model and clinical model; AUC, area under the receiver operating characteristic curve; Sen, sensitivity; Spe, specificity; PPV, positive predictive value; NPV, negative predictive value; and ACC, accuracy.

 doi:10.20944/preprints202312.2320.v1

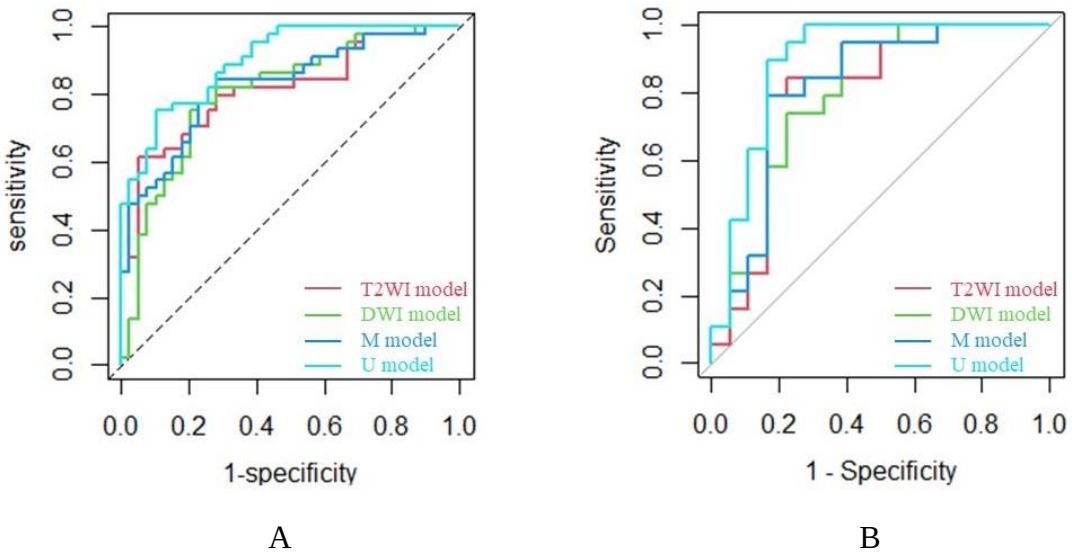

A B

Figure 6. Receiver operating characteristic (ROC) curves show the predictive performance of the T2WI model, the DWI model, the M model, and the U model for CRLM in the training (A) and validation (B) groups.

3. Discussion

Radiomics aims to extract large amounts of high-dimensional data from traditional imaging sequences to mine the underlying pathophysiological information at the microscopic level [26–28] and has demonstrated important roles in diagnosing and treating tumors [29–32]. Most existing studies on the radiomic prediction of CRLM are based on imaging data from the liver parenchyma [33–36]; few studies have used radiomic models based on baseline MRI of the primary lesion in CRC patients to predict CRLM. Liang et al. [37] constructed a radiomics prediction model based on MRI T2WI and venous-phase images of the primary lesion in RC. The results showed that the baseline MRI-omics model based on primary lesion images had predictive potential for LM. Liu et al. [16] established a prediction model using the T2W images of 127 RC patients combined with the levels of tumor markers CEA and CA19-9, which showed good performance in predicting LM. However, none of these studies investigated the role of fine-annotated key sequences (such as DWI) in CRC. Recently, Li et al. [38] reported the effectiveness of radiomics based on multiparametric MRI of first-diagnosed rectal cancer patients in predicting LM in rectal cancer patients. The results showed that the area under the curve (AUC) values of the optimal single sequence model were 0.861 in the training cohort and 0.844 in the validation cohort. Similarly, the AUC values of the DWI+HD T2WI joint model were 0.896 in the training cohort and 0.889 in the validation cohort. The integration of radiomic features into the clinical model improved the predictive performance, with AUC values of 0.916 in the training cohort and 0.911 in the validation cohort. In this study, based on the preoperative baseline T2W and DWI radiomic characteristics of the primary CRC lesion, we created a T2WI model, a DWI model and a T2W+DWI model (M model) and integrated all optimal imaging characteristics and clinical risk factors to establish a clinical-radiomic joint model (U model) to predict CRLM. The results showed that the predictive performance of the T2WI + DWI joint model was better than that of the T2WI or DWI model alone, while the joint clinical-radiomics model had the best predictive performance. The results of this study are consistent with those of Li et al [31].

In addition, these data showed that CEA and CA19-9 levels are independent clinical risk factors for CRLM, which is consistent with the findings of Zhu et al. [39] and Zhang et al. [40]. Li et al. [41–43] reported that TNM stage was a risk factor for CRLM. However, in the present study, there was no difference in the T or N stage of CRC patients between the liver metastasis group and the group without liver metastasis, which may be related to the small sample size of this study.

 doi:10.20944/preprints202312.2320.v1

This study has the following limitations. (1) This was a retrospective study with a small sample size. A prospective study with a large sample should be conducted in the future for further validation. (2) This study used single-center data and lacked external validation. Integrating data from multiple sources can capture more accurate information, resulting in more robust predictions [26]; ideally, model validation should be performed using external data [44]. Multicenter data should also be employed in future studies.

4. Materials and Methods

4.1. Patients

The study subjects included CRC patients who underwent MRI at the Affiliated Hospital of North Sichuan Medical University between June 2016 and August 2022. The patient inclusion criteria were as follows: (1) CRC confirmed by colonoscopy biopsy or postoperative histopathology; (2) no other malignant tumors. (3) complete baseline MR images of good image quality before treatment and no prior antitumor treatment (including radiotherapy, chemotherapy, chemoradiotherapy, or surgery) before the baseline MR examination. (4) follow-up for CRC for a minimum of 1 year. During the follow-up period and at least 1 year after the diagnosis of the primary lesion, patients underwent enhanced CT, MRI or ultrasound examination of the whole abdomen (or upper abdomen) to determine whether they had LM. The exclusion criteria were as follows: (1) histopathologically confirmed mucinous adenocarcinoma (because of the poor prognosis and high risk of developing MLM) (4 patients in the LM group and 14 patients in the no LM group); (2) incomplete imaging data or images of insufficient quality for image segmentation (31 patients in the LM group and 41 patients in the no LM group); (3) primary CRC lesions of insufficient size or lacking clear outlines on MR images (5 patients in the LM group and 5 patients in the no LM group). This group of LM patients was diagnosed by liver biopsy, pathological examination of surgical resection, enhanced CT/MRI or ultrasound examination for typical metastasis features. A total of 220 patients were recruited, and 120 patients were eventually included in this study (Figure 1).

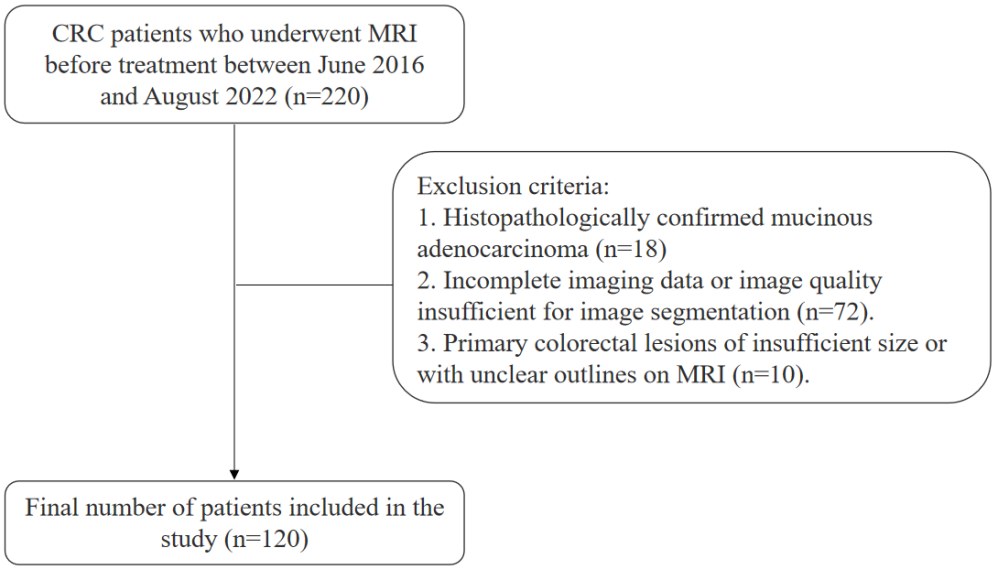

Figure 1. Flowchart of patient enrollment.

The following clinical data were collected from the patients: sex, age, pathological results, MRI T stage, MRI N stage, CEA level and CA19-9 level. MRI TN staging was performed according to the 8th edition of the TNM staging system of the American Cancer Society [45]. The interval between the collection of blood samples for the detection of preoperative CEA and CA19-9 levels and the baseline MRI examination was not more than 2 weeks.

 doi:10.20944/preprints202312.2320.v1

4.2. MRI acquisition

In this study, a standardized rectangular cancer MRI scan protocol was employed with a Discovery 750 3.0T superconducting MRI scanner with 32-channel phased-array surface coils. All patients fasted 4 h before examination, and a glycerol enema (20 mL of glycerol) was used to cleanse the intestinal tract before the examination. Anisodamine or scopolamine (20 mg) was intramuscularly injected half an hour before the examination (none of the patients presented with contraindications before the injection) to prevent movement artifacts caused by physiological peristalsis of the gastrointestinal tract, bladder and other organs. Acquisition sequences included standard sagittal or coronal T2W images without fat compression, (oblique) axial T2W images without fat compression, and high b-value (b=800) DW images (where the oblique axial view refers to the body position perpendicular to the long axis of the rectal lesion). Standard sagittal or coronal T2W images without fat compression were used to determine the location and boundary of the lesion, and the (oblique) axial T2W and DW images without fat compression were used as region of interest (ROI) annotation sequences (Table 1).

Table 1. (Oblique) axial T_2WI and DWI parameters for colorectal cancer.

Sequence	TR/TE (ms)	ST (mm)	Matrix (mm^2)	FOV (mm^2)	FA (°)
(oblique) axial T_2WI	1700-5050/110-120	4-6	320-384×256	200-360×200-360	90
(oblique) axial DWI	3000-7000/50-80	4-6	128-160×192	340-380×340–380	90

Notes: TR, repetition time; TE, echo time; ST, section thickness; FOV, field of view; FA, flip angle.

4.3. Image segmentation and feature extraction

The open-source software IBEX (β1.0,http://bit.ly/IBEX MDAnderson) was used for ROI annotation. On (oblique) axial T2WI and DWI, the volume of the entire tumor was manually delineated layer by layer along the edge of the lesion as the ROI (Figure 2). Gas in the intestinal lumen, cystic degeneration between the lesion and the normal bowel, necrotic and transitional areas and adipose tissue around the intestinal wall were avoided. The operator was not aware of the basic information of the patient, such as the clinical and pathological results, before the target volume was delineated. Four types of radiomic features, namely, gray-level co-occurrence matrix (GLCM), gray-level run-length matrix (GLRLM), intensity histogram and shape, were extracted using IBEX. Finally, the T2WI and DWI feature datasets were generated.

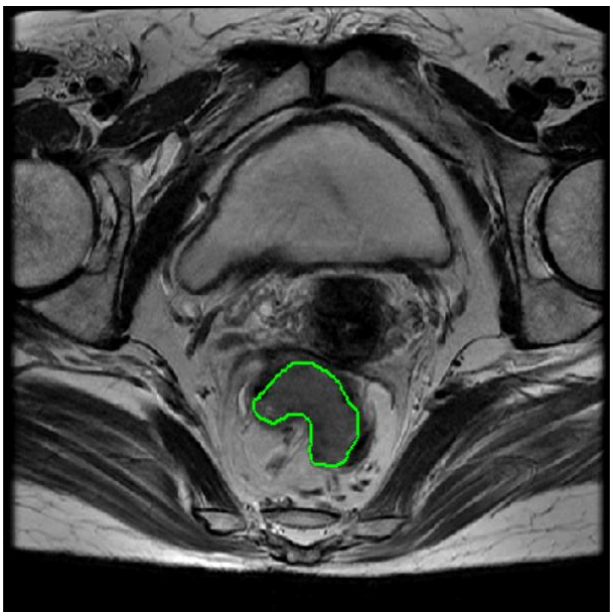

A

 doi:10.20944/preprints202312.2320.v1

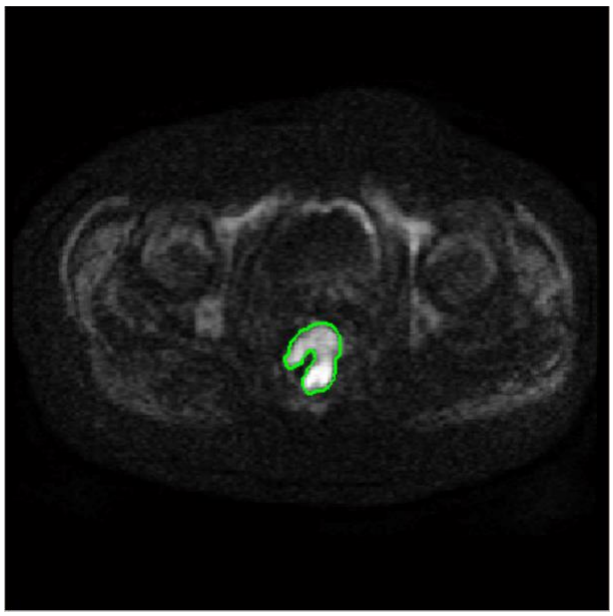

B

Figure 2. On oblique axial T2WI and DWI, the ROI was manually delineated layer by layer along the edge of the rectal cancer lesion. (A) T_2-weighted imaging; (B) Diffusion-weighted imaging.

4.4. Feature dimensionality reduction and selection

For the intraobserver consistency test, radiologist A (with 2 years of work experience) randomly selected approximately 1/3 of the patients from the entire cohort to repeat ROI delineation with a between-delineation interval of at least 1 week. For the interobserver consistency test, radiologists A and B (with 4 years of work experience) each independently delineated the target volume once, and the selected cases were consistent with the intragroup consistency test. The intraclass correlation coefficient (ICC) was used to evaluate the reproducibility of the extracted radiomic features. When the ICC was ≥0.75, the consistency was considered good. Intraobserver and interobserver consistency tests were performed on the dataset generated for each sequence, and features with ICCs <0.75 were excluded. The multicategorical variable MRI TN stage was turned into a dummy variable. The continuous variables CEA and CA19-9 were divided into two groups: the normal group and the elevated group. The mean filling method was used to fill in missing values among the radiomic features to improve sample utilization. To eliminate differences in the index dimension of the data, all the radiomic features were standardized using the z-score statistical method to convert them into feature values with a mean of 0 and a standard deviation of 1.

The features screened by the consistency test were subjected to univariate statistical analysis to further determine the features that were significantly associated with CRLM (P <0.05). Finally, the LASSO regression analysis method was used to select the optimal radiomic features for predicting CRLM risk. Using the 1-standard error (1-SE) method, a 10-fold cross-validation adjustment was used to select the regularization parameter (λ) of the features.

4.5. Model construction and evaluation

Logistic regression was used to construct radiomic prediction models for T2WI and DWI single sequences and for the T2WI-DWI joint model (M). The independent risk factors for predicting CRLM (P <0.05) were screened from among the clinical indicators using univariate and multivariate analyses, and the factors were combined with the T2WI and DWI sequence features to construct a clinical-radiomics joint model (U). The AUC, sensitivity (Sen), specificity (Spe), positive predictive value (PPV), negative predictive value (NPV), accuracy (ACC), and F-1 score were calculated from the confusion matrix and used to assess the predictive performance of the models.

 doi:10.20944/preprints202312.2320.v1

4.6. Statistical methods

R statistical software (4.2.2, https://www.r-project.org/) was used for statistical analysis. For continuous variables, the *Shapiro–Wilk* test was used to determine the normality, and the *Bartlett* test was used to determine the homogeneity of variance. Data satisfying the conditions of normality and homogeneity of variance were analyzed with the independent sample *t* test; otherwise, the *Mann–Whitney U* test was used, and in both cases, the mean value is used to describe the data. Categorical variables were analyzed using the chi-square test and are presented as percentiles. A two-sided *P* value <0.05 was considered to indicate statistical significance.

5. Conclusions

The radiomic model based on features from the T2WI and DWI sequences of CRC primary lesions could predict CRLM well; the combination of clinically independent risk factors and radiomic features further improved the predictive performance of the model.

Supplementary Materials: The following supporting information can be downloaded at the website of this paper posted on Preprints.org.

References

1. Martinou E., Moller-Levet C., Karamanis D., Bagwan I., Angelidi AM. HOXB9 Overexpression Promotes Colorectal Cancer Progression and Is Associated with Worse Survival in Liver Resection Patients for Colorectal Liver Metastases. Int J Mol Sci 2022;23(4): 2281.
2. Delattre JF., Selcen Oguz Erdogan A., Cohen R., Shi Q., Emile JF., Taieb J., Tabernero J., André T., Meyerhardt JA., Nagtegaal ID., et al. A comprehensive overview of tumour deposits in colorectal cancer: Towards a next TNM classification. Cancer Treat Rev 2022;103: 102325.
3. Akgül Ö., Çetinkaya E., Ersöz Ş., Tez M. Role of surgery in colorectal cancer liver metastases. World J Gastroenterol 2014;20(20): 6113-22.
4. Rada M., Kapelanski-Lamoureux A., Petrillo S., Tabariès S., Siegel P., Reynolds AR., Lazaris A., Metrakos P. Runt related transcription factor-1 plays a central role in vessel co-option of colorectal cancer liver metastases. Commun Biol 2021;4(1): 950.
5. de'Angelis N., Baldini C., Brustia R., Pessaux P., Sommacale D., Laurent A., Le Roy B., Tacher V., Kobeiter H., Luciani A., et al. Surgical and regional treatments for colorectal cancer metastases in older patients: A systematic review and meta-analysis. PLoS One 2020;15(4): e0230914.
6. Engstrand J., Nilsson H., Strömberg C., Jonas E., Freedman J. Colorectal cancer liver metastases-a population-based study on incidence, management and survival. BMC Cancer 2018;18(1): 78.
7. Poturnajova M., Furielova T., Balintova S., Schmidtova S., Kucerova L., Matuskova M. Molecular features and gene expression signature of metastatic colorectal cancer (Review). Oncol Rep 2021;45(4): 10.
8. Bhullar DS., Barriuso J., Mullamitha S., Saunders MP., O'Dwyer ST., Aziz O. Biomarker concordance between primary colorectal cancer and its metastases. EBioMedicine 2019;40: 363-374.
9. Xu J., Fan J., Qin X., Cai J., Gu J., Wang S., Wang X., Zhang S., Zhang Z., China CRLM Guideline Group. Chinese guidelines for the diagnosis and comprehensive treatment of colorectal liver metastases (version 2018). J Cancer Res Clin Oncol 2019;145(3): 725-736.
10. Ren L., Zhu D., Benson AB 3rd., Nordlinger B., Koehne CH., Delaney CP., Kerr D., Lenz HJ., Fan J., Wang J., et al. Shanghai international consensus on diagnosis and comprehensive treatment of colorectal liver metastases (version 2019). Eur J Surg Oncol 2020;46(6): 955-966.
11. Loo JM., Scherl A., Nguyen A., Man FY., Weinberg E., Zeng Z., Saltz L., Paty PB., Tavazoie SF. Extracellular metabolic energetics can promote cancer progression. Cell 2015;160(3): 393-406.
12. Li Y., Eresen A., Shangguan J., Yang J., Lu Y., Chen D., Wang J., Velichko Y., Yaghmai V., Zhang Z. Establishment of a new non-invasive imaging prediction model for liver metastasis in colon cancer. Am J Cancer Res 2019;9(11): 2482-2492.
13. Kijima S., Sasaki T., Nagata K., Utano K., Lefor AT., Sugimoto H. Preoperative evaluation of colorectal cancer using CT colonography, MRI, and PET/CT. World J Gastroenterol 2014;20:16964–16975.
14. Gaitanidis A., Alevizakos M., Tsaroucha A., Tsalikidis C., Pitiakoudis M. Predictive Nomograms for Synchronous Distant Metastasis in Rectal Cancer. J Gastrointest Surg 2018;22(7): 1268-1276.

 doi:10.20944/preprints202312.2320.v1

15. Wu JB., Sarmiento AL., Fiset PO., Lazaris A., Metrakos P., Petrillo S., Gao ZH. Histologic features and genomic alterations of primary colorectal adenocarcinoma predict growth patterns of liver metastasis. World J Gastroenterol 2019;25(26): 3408-3425.
16. Liu M., Ma X., Shen F., Xia Y., Jia Y., Lu J. MRI-based radiomics nomogram to predict synchronous liver metastasis in primary rectal cancer patients. Cancer Med 2020;9(14): 5155-5163.
17. Lambin P., Rios-Velazquez E., Leijenaar R., Carvalho S., van Stiphout RG., Granton P., Zegers CM., Gillies R., Boellard R., Dekker A., et al. Radiomics: extracting more information from medical images using advanced feature analysis. Eur J Cancer 2012;48(4): 441-446.
18. Gillies RJ., Kinahan PE., Hricak H. Radiomics: Images Are More than Pictures, They Are Data. Radiology 2016;278(2): 563-77.
19. Zhang X., Zhang Y., Zhang G., Qiu X., Tan W., Yin X., Liao L. Deep Learning With Radiomics for Disease Diagnosis and Treatment: Challenges and Potential. Front Oncol 2022;12: 773840.
20. Mayerhoefer ME., Materka A., Langs G., Häggström I., Szczypiński P., Gibbs P., Cook G. Introduction to Radiomics. J Nucl Med 2020;61(4): 488-495.
21. Yip SS., Aerts HJ. Applications and limitations of radiomics. Phys Med Biol 2016;61(13): R150-66.
22. Avanzo M., Wei L., Stancanello J., Vallières M., Rao A., Morin O., Mattonen SA., El Naqa I. Machine and deep learning methods for radiomics. Med Phys 2020;47(5): e185-e202.
23. Liu N., Wu Y., Tao Y., Zheng J., Huang X., Yang L., Zhang X. Differentiation of Hepatocellular Carcinoma from Intrahepatic Cholangiocarcinoma through MRI Radiomics. Cancers (Basel) 2023;15(22):5373.
24. Gong XQ., Liu N., Tao YY., Li L., Li ZM., Yang L., Zhang XM. Radiomics models based on multisequence MRI for predicting PD-1/PD-L1 expression in hepatocellular carcinoma. Sci Rep 2023;13(1):7710.
25. Mao Q., Zhou MT., Zhao ZP., Liu N., Yang L., Zhang XM. Role of radiomics in the diagnosis and treatment of gastrointestinal cancer. World J Gastroenterol 2022;28(42):6002-6016.
26. Alshohoumi F., Al-Hamdani A., Hedjam R., AlAbdulsalam A., Al Zaabi A. A Review of Radiomics in Predicting Therapeutic Response in Colorectal Liver Metastases: From Traditional to Artificial Intelligence Techniques. Healthcare (Basel) 2022;10(10): 2075.
27. Staal FCR., Taghavi M., van der Reijd DJ., Gomez FM., Imani F., Klompenhouwer EG., Meek D., Roberti S., de Boer M., Lambregts DMJ., et al. Predicting local tumour progression after ablation for colorectal liver metastases: CT-based radiomics of the ablation zone. Eur J Radiol 2021;141: 109773.
28. Tharmaseelan H., Hertel A., Tollens F., Rink J., Woźnicki P., Haselmann V., Ayx I., Nörenberg D., Schoenberg SO., Froelich MF. Identification of CT Imaging Phenotypes of Colorectal Liver Metastases from Radiomics Signatures-Towards Assessment of Interlesional Tumor Heterogeneity. Cancers (Basel) 2022;14(7): 1646.
29. de la Pinta C., Castillo ME., Collado M., Galindo-Pumariño C., Peña C. Radiogenomics: Hunting Down Liver Metastasis in Colorectal Cancer Patients. Cancers (Basel) 2021;13(21): 5547.
30. Han Y., Chai F., Wei J., Yue Y., Cheng J., Gu D., Zhang Y., Tong T., Sheng W., Hong N., et al. Identification of Predominant Histopathological Growth Patterns of Colorectal Liver Metastasis by Multi-Habitat and Multi-Sequence Based Radiomics Analysis. Front Oncol 2020;10: 1363.
31. Granata V., Fusco R., De Muzio F., Cutolo C., Setola SV., Dell' Aversana F., Ottaiano A., Avallone A., Nasti G., Grassi F., et al. Contrast MR-Based Radiomics and Machine Learning Analysis to Assess Clinical Outcomes following Liver Resection in Colorectal Liver Metastases: A Preliminary Study. Cancers (Basel) 2022;14(5): 1110.
32. Shi R., Chen W., Yang B., Qu J., Cheng Y., Zhu Z., Gao Y., Wang Q., Liu Y., Li Z., et al. Prediction of KRAS, NRAS and BRAF status in colorectal cancer patients with liver metastasis using a deep artificial neural network based on radiomics and semantic features. Am J Cancer Res 2020;10(12): 4513-4526.
33. Granata V., Fusco R., De Muzio F., Cutolo C., Setola SV., Dell'Aversana F., Grassi F., Belli A., Silvestro L., Ottaiano A., et al. Radiomics and machine learning analysis based on magnetic resonance imaging in the assessment of liver mucinous colorectal metastases. Radiol Med 2022;127(7): 763-772.
34. Taghavi M., Trebeschi S., Simões R., Meek DB., Beckers RCJ., Lambregts DMJ., Verhoef C., Houwers JB., van der Heide UA., Beets-Tan RGH., et al. Machine learning-based analysis of CT radiomics model for prediction of colorectal metachronous liver metastases. AbdomRadiol (NY) 2021;46(1): 249-256.
35. Becker AS., Schneider MA., Wurnig MC., Wagner M., Clavien PA., Boss A. Radiomics of liver MRI predict metastases in mice. EurRadiol Exp 2018;2(1): 11.
36. Rocca A., Brunese MC., Santone A., Avella P., Bianco P., Scacchi A., Scaglione M., Bellifemine F., Danzi R.,

 doi:10.20944/preprints202312.2320.v1

Varriano G., et al. Early Diagnosis of Liver Metastases from Colorectal Cancer through CT Radiomics and Formal Methods: A Pilot Study. J Clin Med 2021;11(1): 31.

37. Liang M., Cai Z., Zhang H., Huang C., Meng Y., Zhao L., Li D., Ma X., Zhao X. Machine Learning-based Analysis of Rectal Cancer MRI Radiomics for Prediction of Metachronous Liver Metastasis. Acad Radiol 2019;26(11): 1495-1504.
38. Li ZF., Kang LQ., Liu FH., Zhao M., Guo SY., Lu S., Quan S. Radiomics based on preoperative rectal cancer MRI to predict the metachronous liver metastasis. Abdom Radiol (NY) 2023;48(3): 833-843.
39. Zhu HQ., Wang DY., Xu LS., Chen JL., Chu EW., Zhou CJ. Diagnostic value of an enhanced MRI combined with serum CEA, CA19-9, CA125 and CA72-4 in the liver metastasis of colorectal cancer. World J Surg Oncol 2022;20(1): 401.
40. Zhang D., Yu M., Xu T., Xiong B. Predictive value of serum CEA, CA19-9 and CA125 in diagnosis of colorectal liver metastasis in Chinese population. Hepatogastroenterology 2013;60(126): 1297-301.
41. Li Y., Gong J., Shen X., Li M., Zhang H., Feng F., Tong T. Assessment of Primary Colorectal Cancer CT Radiomics to Predict Metachronous Liver Metastasis. Front Oncol 2022;12: 861892.
42. Lee S., Choe EK., Kim SY., Kim HS., Park KJ., Kim D. Liver imaging features by convolutional neural network to predict the metachronous liver metastasis in stage I-III colorectal cancer patients based on preoperative abdominal CT scan. BMC Bioinformatics 2020;21(Suppl 13): 382.
43. Landreau P., Drouillard A., Launoy G., Ortega-Deballon P., Jooste V., Lepage C., Faivre J., Facy O., Bouvier AM. Incidence and survival in late liver metastases of colorectal cancer. J Gastroenterol Hepatol 2015;30(1): 82-5.
44. Huang EP., O'Connor JPB., McShane LM., Giger ML., Lambin P., Kinahan PE., Siegel EL., Shankar LK. Criteria for the translation of radiomics into clinically useful tests. Nat Rev Clin Oncol 2022: 1–14.
45. Amin MB., Greene FL., Edge SB., Compton CC., Gershenwald JE., Brookland RK., Meyer L., Gress DM., Byrd DR., Winchester DP. The Eighth Edition AJCC Cancer Staging Manual: Continuing to build a bridge from a population-based to a more "personalized" approach to cancer staging. CA Cancer J Clin 2017;67(2):93-99.